FR8403367

2

institut de physique nucléaire
LABORATOIRE ASSOCIÉ A L'IN2P3

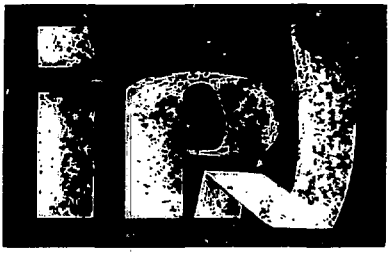

IPNO-DRE-83-32
83-32

SOLENO, A SUPERCONDUCTING SOLENOIDAL COIL USED AS A SPECTROMETER FOR NUCLEAR CHARGED PARTICLES STUDIES AROUND ZERO DEGREE.

Jean-Paul SCHAPIRA, Faïçal AZAIEZ, Simone FORTIER, Sydney GALES, Eid HOURANI, Jaana KUMPULAINEN and Jean-Marie MAISON

UNIVERSITÉ PARIS SUD

IPNO-DRE-8332

SOLENO, A SUPERCONDUCTING SOLENOIDAL COIL USED AS A SPECTROMETER FOR NUCLEAR CHARGED PARTICLES STUDIES AROUND ZERO DEGREE.

Jean-Paul SCHAPIRA, Faiçal AZAIEZ, Simone FORTIER, Sydney GALES, Eid HOURANI, Jaana KUMPULAINEN and Jean-Marie MAISON

(submitted for publication in Nuclear Instruments and Methods)

SOLENO, a superconducting solenoidal coil used as a spectrometer for nuclear charged particles studies around zero degree.

Jean-Paul SCHAPIRA, Faiçal AZAIEZ, Simone FORTIER,
Sydney GALES, Eid HOURANI, Jaana KUMPULAINEN*
and Jean-Marie MAISON

Institut de Physique Nucléaire, B.P. n°1, 91406 Orsay, France.

A new type of spectrometer for nuclear charged particles studies has been designed and built near the 13 MV Tandem accelerator of the Institut de Physique Nucléaire at Orsay (France). It makes use of the focusing properties of an axial magnetic field of 3.17 Teslas (at maximum value) produced by a superconducting solenoidal coil. The basic properties of such a device are the followings : true azimuthal symmetry, large angular acceptance (up to 10°), reduced geometrical and mechanical aberrations leading to a bandwith of 5% in magnetic rigidity. Associated with a system of detection of small size, this spectrometer is now used around zero degree for coincidence experiments and to collect and identify in mass, fusion evaporation residues. In this later case, the system is operating like a recoil mass separator (RMS).

---

* On leave from the University of Jyväskylä, SF-40100 Jyväskylä, Finland

1 - INTRODUCTION

For more than few decades, optical properties of solenoidal coils have been widely studied and used in electron microscopes [1,2], β-ray spectrometers [3,4] and more recently in the design of electron guns associated with multi-charged heavy ion sources [5]. Recent development in superconducting technology makes attractive the use of superconducting solenoids for producing high longitudinal magnetic fields needed to manipulate accelerator beam properties, sometimes in a more efficient way than whith classical magnetic focusing elements [6,7,8]. On the other hand, little attention has been paid up to now to the possibility of using these devices as heavy charged particle spectrometers [9-12].

For this purpose, a superconducting solenoidal spectrometer, under the name SOLENO has been proposed [9], designed and built at the Institut de Physique Nucléaire, Orsay. The first part of SOLENO, consisting of one coil, is now under operation [10] since September 1982 near the 13 MV Tandem accelerator of Orsay and is described in this article (see Fig. 1). SOLENO will be completed in 1984 with a second identical coil, in order to extend its capabilities for time of flight experiments and to particles of larger magnetic rigidity.

2 - GENERAL DESCRIPTION

The main characteristic of such a spectrometer is its fully azimuthal symmetry leading to a large solid angle. This property is due in practice to the use of a thin superconducting wire, which can simply be winded around a cylindrical tube without significant mechanical aberrations as compared with a conventional solenoid producing the same magnetic field. Because of the specific trajectory properties (Busch's theorem), good focusing properties are expected with small geometrical aberration effects [1,7]. Therefore the detector located in the image region can be chosen of moderate size (diameter typically of the order of 10-20 mm) and still collect ions emitted from the target within a large angular range. In order to achieve good solid angle (94 msr in the standard case of SOLENO), the target must be as near as possible to the entrance of the spectrometer and the inner vacuum tube of sufficient diameter to let particles go through the system. Therefore this type of coil has usually a large diameter to length ratio and need an iron shield around in order to protect both the target and detector regions from an important stray magnetic field.

The spectrometer SOLENO has been specially designed to operate at zero degree of the direction of the beam stopped in a Faraday cup at the entrance of the system. In this set-up, SOLENO is now used for two types of experiments. First for true double angular correlation studies in the so-called Litherland and Ferguson geometry [13], extending the previous triplet system [14] to lower cross sections because of its larger solid angle. Secondly the spectrometer is used as a fast and efficient collector of fusion-evaporation products from light compound systems of mass A less than 50, region for which SOLENO in connection with a time of flight and energy measurements, is well adapted.

Figure 2 shows the general set up of SOLENO with the basic devices. The Faraday cup made of graphite, is maintained by 6 titanium wires of 0.2 mm diameter. It limits the minimum angle of detection to 1 degree when the target is located at 60 cm from the front edge of the coil. Five values of the minimum angle of acceptance can be set by inserting stainless steel obturators with rounded and polished edges (in order to reduce scattering effects), in front of the Faraday cup. On the other hand the maximum value can continuously be adjusted with a diaphragm system of 12 sliding slides operating like a photographic iris. The technical characteristics of SOLENO itself are reported in table I, and described in reference 15. For safety reason, the inner vacuum tube of a diameter of 0.36 m, is at room temperature. On the other hand the 3V, 375A power supply is permanently connected to the superconducting coil in order to easily adjust the current to a preset value.

3 - MAGNETIC FIELD STUDIES

Because of azimuthal symmetry, the magnetic field $\vec{B}$ has only two components B_r and B_z deriving from the potential vector $\vec{A} = (o, o, A_\varphi = A)$, expressed in the usual cylindrical coordinates system (r, z, φ) (see e.g. ref. 1). The magnetic field has been calculated with the code TRIM [16], which takes into account the exact geometry of the coil and the iron shield (Fig. 3), designed in such a way to prevent saturation effects at maximum excitation current in the coil (375 A). In this configuration the stray field is minimized at the target and detector locations, as can be seen on figure 4, and the optical properties become independent of the current setting. The iron shield has been cut around the median plane to allow clearance for the liquid helium pipe and the various connections, all around 2π in order to preserve azimuthal symmetry. The median planes of the coil and of the iron shield do not coincide exactly (15 mm difference), which explains a slight lack of symmetry around the median plane of the latter one (Fig. 3), taken as the origin z = 0 of the polar axis.

These calculations reproduce, with an accuracy of the order of one percent, the actual axial field $B(z) = B_z$ $(r = o, z)$ measured with an Hall effect probe. The polar axis has been determined with a radial probe measuring the radial component B_r at various angular settings around the geometrical axis (beam axis). An off set of the order of 2 mm at the entrance and the exit of SOLENO, with respect to the geometrical axis has been founded and shown to be due to the proximity of iron pieces. This small lack of symmetry has no significant effect on the optical properties of SOLENO, and was taken into account to locate the detector in the image region.

4 - OPTICAL PROPERTIES OF SOLENO

4.1. - General outline

The optical characteristics of a solenoidal coil spectrometer like SOLENO are defined by a set of relevant parameters as follows :

a) the maximum $B\rho$ achievable for a certain geometrical set-up of the target and the detector, at maximum current I = 375 A.

b) the maximum angle of acceptance for the same geometrical conditions and for a certain size of the detector.

c) the linear magnification, valid for paraxial rays (Gauss approximation)

d) the spherical aberration which determines the size of the image produced at the detector plane by a bundle of rays emitted from a point source (target) within a certain angular range and for a definite value of $B\rho$.

e) the transmission curve $\alpha = f(B\rho/\overline{B\rho})$ which relates the angular acceptance to the $B\rho$ of the particles, when the magnetic field has been set in order to optimize the solid angle for the central value $\overline{B\rho}$. This curve depends on the geometrical set-up and on the detector size.

f) the length of a trajectory between target and detector versus the angle of emission, which determines the degree of isochronism relevant for time of flight experiments.

All these quantities can be deduced from the general equations of motion for an ion emitted from the target located at $z = z_0$, with definite initial conditions : magnetic rigidity $B\rho$, distance r_0 from the polar axis, angle α with the polar axis and azimuthal angle ψ (this angle ψ is different from zero for skew rays emitted from the target with $r_0 \neq 0$).

Two basic geometries have been considered in this study :

i) The geometry A takes full advantage of the large diameter 0.36 m of the vacuum tube to achieve the largest solid angle. It is defined by the target and the detector being the nearest as possible to the entrance and exit faces of SOLENO ($Z_0 = -0.96$ m, $Z_I = 1.0$ m).

ii) The geometry B ($Z_0 = -1.18$ m and $Z_I = 1.375$ m) has been used for the two types experiments discussed in sections 5 and 6, because it allows a larger $B\rho$ value (necessary for focusing 42 MeV α) and a longer flight path (for better mass separation). Of course the angular acceptance is lower in this case.

The optical properties have been calculated in these two geometries, and some of them measured with an α-source only in geometry B.

4.2. – **Optical properties calculations**

Because of azimuthal symmetry, one equation relating the elongation $r(z)$ to the position z is sufficient to calculate the optical characteristics listed above and can be written in the convenient form [9] :

$$\frac{1-\eta^2}{1+r'^2} \cdot r'' - \eta \frac{\partial \eta}{\partial z} r' + \eta \frac{\partial \eta}{\partial r} = 0 \qquad (1)$$

where ' denotes derivation with respect to z, and η the quantity :

$$\eta = \frac{A}{(B\rho)} - \frac{r_0}{r} \left(\sin\alpha \sin\psi + \frac{A_0}{B\rho} \right) \qquad (2)$$

A_0 being the potential vector at the origin $z = z_0$.

The Gauss approximation for an ion leaving the target position on the axis ($r_o = o$), is obtained from eq. (1) by neglecting r' and taking only the first term in the Taylor expansion of A in r. It leads to the well-known equation :

$$r'' = -\left(\frac{B(z)}{2(B\rho)}\right)^2 r \qquad (3)$$

B(z) is the magnetic field along the axis. The two particular solutions of (3) $r_\alpha(z)$ ($r_o = o$, $r'_o = 1$) and $r_\gamma(z)$ ($r_o = 1$, $r'_o = 0$) define first order quantities such as the position Z_G of the plane of Gauss focus, the focal length, the linear magnification M_L. On the other hand, the third order spherical aberration coefficient C_3 defining the radius $\rho_3 = C_3\alpha^3$ of the image at the plane of Gauss focus (for a point source) can be derived from the Glaser equation [1] :

$$C_3 = \frac{M_L}{12} \int_{Z_o}^{Z_G} (16\,K^4 + 5\,K'^2 - KK'')\, r_\alpha^4 \, dz \qquad (4)$$

where $K(z) = \frac{B(z)}{2(B\rho)}$. The detector is located at the plane of best focus, or of least confusion [1,9]. In the case of the third approximation, the elongation at this plane, of a bundle of rays emitted with $\alpha < \alpha_{max}$, is minimum, and equal to :

$$\rho = \frac{C_3}{4}\,\alpha_{max}^3 + M_L \cdot \phi/2 \qquad (5)$$

where ϕ is the diameter of the source. It is easy to show that this plane is located at the focus point for a ray emitted with $\alpha = \alpha_{max} \cdot \frac{\sqrt{3}}{2}$ and is ahead of the plane of Gauss focus by a quantity equal $\frac{3}{4}\left|C_3\right|\alpha_m^2$ (ref. [1,9]).

The degree of isochronism can be expressed in terms of the ratio $\Delta\ell/\ell_o / \alpha^2$, which can be shown to be roughly independent of α for $\alpha << 1$ (ref. 9).

A ray trace program SOLEN, developped at Orsay, solves eq. (1) exactly in the actual magnetic field generated by the program TRIM. In the practical case of SOLENO, a Taylor expansion of the potential vector A up to the third order in r (ref. 9) :

$$A = \frac{r}{2} B(z) - \frac{r^3}{16} B''(z), \qquad (6)$$

is sufficient to reproduce the ray trace program results as well as the α-source measurements. The results reported in tab. 2 have been obtained in this approximation, using a program under the name GAUSS, developped at Orsay, with the main advantage to be much faster than SOLEN.

4.3. - Alpha-rays measurements and transmission curves

For geometry B, the current setting of SOLENO which brings the circle of least confusion at the detector location, has been obtained using a two dimensional position sensitive detector (so called X-Y detector). The maximum $B\rho$ value, at I = 375 A, is the value for which the X-Y image in the detector has the minimum size. Measurements have been achieved using the 5.486 MeV alpha-rays from an ^{241}Am source. Different images, showing a fairly good azimuthal symmetry are reported on figure 5. The minimum size as well as the current corresponding to $B\rho$ = 0.340 T x m (E_α = 5.486 MeV), leading to $B\rho_{max}$ = (0.944 ± 0.001) T x m at I = 375 A, are quiet well reproduced by the theoretical calculations (see tab. 2).

The transmission curve obtained with an ^{241}Am source, using a 250 mm^2 circular detector (fig. 6), are also fairly well reproduced by a third order calculation, taking into account the entrance and exit diameter of SOLENO. A bandwith of the order of 5% in $\overline{B\rho}$ is achieved with geometry B.

For a certain $B\rho$ setting, particles with certain smaller $B\rho$ values are refocused onto the detector [9]. These spurious trajectories can be stopped inside the spectrometer, because they cross at least one time the polar axis before reaching the detector. A cylindrical baffle located on the axis around the median plane achieve this goal.

The linear magnification M_L and the angle of rotation of the meridian plane, have been roughly estimated by detecting in the X-Y detector the displacement in distance and angle of the image, when the alpha source was translated from its original position.

5 - USE OF SOLENO AROUND ZERO DEGREE FOR COINCIDENCE EXPERIMENTS

Azimuthal symmetry, large solid angle (94 msr in geom. A) and a bandwidth in energy of the order of 10%, allow coincidence experiments for two-body reaction to be undertaken in an efficient way. Because SOLENO is located around the beam direction, only two directions are involved in the angular correlation : the beam axis (a) or (b) and the direction of detection of the secondary particles or gamma-rays (c) emitted from the target, according to the well known sequence : A(a,b) B*(c) C. The correlation measured is between b and c. This method, called Method II of Litherland and Ferguson [13], is known to be a useful tool for spins, multipolarity mixing ratio assignment and level schemes determination.

The γ-decay properties of deeply bound hole states in ^{111}Sn, excited in the $^{112}Sn(^{3}He,\alpha)^{111}Sn$ reaction at 36 MeV incident energy, have been recently studied with SOLENO by measuring the γ-ray spectrum in coincidence with the alpha particles. These were detected between 2.6° and 6° (28 msr) with a surface barrier detector (area = 250 mm^2, thickness = 2000 μ). A typical energy spectrum is shown in figure 7 with a $B\rho$ setting of 0.930 T x m = 1.24 $B\rho$ (beam). The elastic peak is negligible in this case.

The important caracteristic of a system such as SOLENO which detects at small angle, is its ability to reject scattered beam, the direct beam being stopped in a Faraday cup (Fig. 2). This property can be expressed as the ratio of elastic events detected in the detector to the number of scattered particles entering in SOLENO. Because this ratio increases when the current setting gets nearer to $\overline{B\rho}$ = $B\rho$ (beam), the beam rejection capability can be also defined by the minimum value of r = $\overline{B\rho}/B\rho$ (beam) at which the counting rate in the detector is still at a reasonnable level. In the case of figure 7 (r = 1.24), the rejection ratio is estimated to be of the order of 5 x 10^{-6}. On the other hand, figure 8 shows four ^{112}Sn + ^{3}He spectra corresponding to different values of the ratio r. As expected, the elastic peak increases when r$\rightarrow$1. One observes that it is still possible to work at r = 1.10, at least with a beam of small emittance like the one delivered by a Tandem accelerator. It is worth pointing out that these performances depend critically on the beam quality and on the possibility to eliminate beam edges. In this respect, the introduction of a baffle inside SOLENO, as mentionned in sect. 4.2., will undoubtely improve the actual performances.

6 - USE OF SOLENO AS RECOIL MASS SEPARATOR (R.M.S)

6.1. - General outline

Even in its one coil version, SOLENO is particularly suitable as recoil mass separator for A < 50 fusion evaporation residues produced at Tandem energies. This is due to its large angular acceptance, well adapted to the angular distribution of most fusion products peaked around few degrees (typically 5°). The energy spectrum of these is also well adapted to the various $B\rho$ settings of SOLENO for which good scattered beam rejection can be achieved. In this set-up, SOLENO acts merely as a $B\rho$ filter with a large solid angle. Mass identification must be achieved by energy and time of flight measurements. The precision ΔE on the energy measurement with a conventional semi conductor is typically of the order of 1% and is good enough for the mass values A < 50. The main advantage of SOLENO is its very good isochronism (dependence of the length of a trajectory with the angle of emission), because in contrast with deflecting systems without compensation [17] or position sensitive detectors, full azimuthal symmetry is achieved with SOLENO and length fluctuation with angle has a smaller dependence on solid angle [9]. As a consequence, SOLENO appears as a large solid angle device in which velocity can be measured with few 10^{-3} precision, using the usual time of flight technique. Because of the $B\rho$ bandwidth (5%), the charge state Q can also be obtained with this accuracy. In its simplicity of operation and design, SOLENO appears to be very different from other R.M.S. described in ref. 17 (e.g. SHIP, Rochester), which are used to collect fusion products emitted very near to 0 degree and for which therefore beam rejection becomes a major problem.

6.2. - Preliminary results concerning the reaction $^{16}O+^{12}C$ at 100 MeV incident energy (^{16}O beam)

These features have been evidenced in the fusion-evaporation $^{16}O + ^{12}C$ reaction at 100 MeV incident energy where mass and charge state identification has been observed for A < 26 and Q < 13. In order to get the best mass resolution, target and detector have been set further apart in a geometry slightly different of the geometry B. The start signal for the time of flight measurement was produced in a thin scintillator film located in front of the entrance of SOLENO. Table 3 summarizes the experimental conditions of this experiment. The overall mass resolution has been deduced in the following way : in the bidimensional plot (t, E), one can measure the relative width Δt_g of each time peak associated with a given mass of a definite energy. It is then

easy to show that the mass resolution $\Delta A/A$ is equal to $\Delta t_g/t_g$. One has obtained Δt_g = 1.2 ns leading to ΔA = 1/50. The bidimensional plot (t, E) can be transformed to a plot (Q, A) using the well known transformations :

$$A = k_1 \; E \; t^2$$
$$Q = k_2 \; E \; t$$

where k_1 and k_2 depend on the experimental conditions. On this plot, one effectively distinguishes clearly most of the fusion products together with the $^{12}C^{5,6+}$ and $^{16}O^{6,7,8+}$ ions (see figure 9). A total mass spectrum is shown on figure 10. With the present improvement of the detection system, an even clearer mass separation will be achieved, even in the case of the one coil configuration.

7 – CONCLUSION

The first experimental results show the advantages of using a solenoidal magnetic coil at least for the two types of experiments discussed here. Other studies with such a device can be considered, like for example angular distributions at very small angle with good angular resolution and large solid angle, by making use of the azimuthal symmetry. Because of their small cross sections, exotic reactions could be studied in this way.

The extension of SOLENO to two coils will also widen the scope of possible experiments due to improved characteristics : smaller geometrical aberrations leading to "flatter" transmission curves, larger solid angle together with higher magnetic rigidity and longer flight path for better mass identification.

REFERENCES

1) V.E. GOSSLETT. Introduction to Electron Optics (Oxford 1950)

2) P. GRIVET. Optique Electronique (Bordas 1955)

3) K. SIEGBAHN. Alpha, beta and gamma-ray spectroscopy (North Holland - Publishing Company)

4) I. LINDGREN and W. SCHNEIDER. Nucl. Inst. and Meth. 22 (1963) 48

5) J. ARIANER and R. GELLER. Annual Review of Nuclear Particles Sciences 31 (1981) 15

6) A.H. JAFFREY and TAT KHOE. Nucl. Instrum. and Meth. 121 (1974) 413

7) H. KOYAMA-ITO and L. GRODZINS. Nucl. Instrum. and Meth. 174 (1980) 331

8) J. NOLEN and B. ZEIDMAN. Workshop on high resolution large acceptance spectrometer. ANL/PHY-81-2 (1981)

9) J.P. SCHAPIRA, S. GALES and H. LAURENT. Orsay. Internal report. IPNO-PhN-7921

10) F. AZAIEZ et al.. Proceedings of the International Conference on Nuclear Physics. Florence (Aug. 29 - Sept. 3. 1983) vol. 1, page 733

11) H. LAURENT and J.P. SCHAPIRA. Nucl. Instrum. and Meth. 162 (1979) 181

12) D. JOHNSON. Ed. KASHY and J. NOLEN. Private Communication.

13) A.E. LITHERLAND and A.J. FERGUSON. Can. J. Phys. 39 (1961) 788

14) H. LAURENT, J.P. SCHAPIRA, S. FORTIER, S. GALES and J.M. MAISON. Nucl. Instrum. and Meth. 117 (1974) 17

15) G. LEVY, S. BUHLER, M. KOVALSKI and A. LIEBE. 8th International Conference on Magnet Technology. Grenoble (France), 5-9 Sept. 1983

16) J.S. COLONIAS. TRIM : a magnetostatic computer program for the CDC6600. report UCLA-18439 (1968) (modified version)

17) H.A. ENGE. Nucl. Instrum. and Meth. 186 (1981) 413

LIST OF FIGURES

FIG. 1 : General view of SOLENO

FIG. 2 : General set-up of SOLENO, with its main components (geometry A) :

- A – Target chamber
- B – Box containing five obturators, defining the minimum acceptance angle
- C – Iris, defining the maximum acceptance angle
- D – Faraday cup
- E – Coil (length : 0.75 m, inner diameter : 0.486 m, outer diameter : 0.516 m)
- F – Inner bore, diameter 0.36 m
- G – Iron shield, thickness 0.08 m
- H – Box for cryogenic pumping
- I – Detector chamber

FIG. 3 : Magnetic configuration of SOLENO (TRIM calculation, see § 3)

FIG. 4 : Magnetic field B(z) on axis : (a) actual magnetic field with the iron shield – (b) magnetic field without any iron shield – (c) actual magnetic field measured with an Hall effect probe.

FIG. 5 : Image sizes for different Bρ settings (geometry B), using the 5.48 MeV alpha ray of ^{241}Am and a position sensitive detector, for $1° \leqslant \alpha \leqslant 6.1°$. (a) : $B\rho/\overline{B\rho} = 1.$; (b) : $B\rho/\overline{B\rho} = 1.01$ (size : 13.9 mm). In case (b) the internal circle is due to the Faraday cup.

FIG. 6 : Transmission curve using a 250 mm^2 circular detector, measured with an alpha source (geometry B), and calculated in the third order approximation. In this case : • : limited by the detector size, + : limited by the entrance (6.1°) and o : limited by the exit.

FIG. 7 : $^{3}He + ^{112}Sn$ spectrum at 36 MeV incident energy (see § 5). Target thickness : 350 $\mu g/cm^2$, total integrated charge 70 μC, solid angle : 28 msr ($2.6° < \alpha < 6°$). $\overline{B\rho}$ = 0.930 T x m.

FIG. 8 : Four $^{3}He + ^{112}Sn$ spectra at 36 MeV incident energy, for different current settings of SOLENO.

FIG. 9 : Mass and charge state spectrum in the $^{16}O + ^{12}C$ reaction at 100 MeV incident energy (^{16}O beam).

FIG. 10 Total mass spectrum obtained in the $^{16}O + ^{12}C$ reaction at 100 MeV incident energy (^{16}O beam).

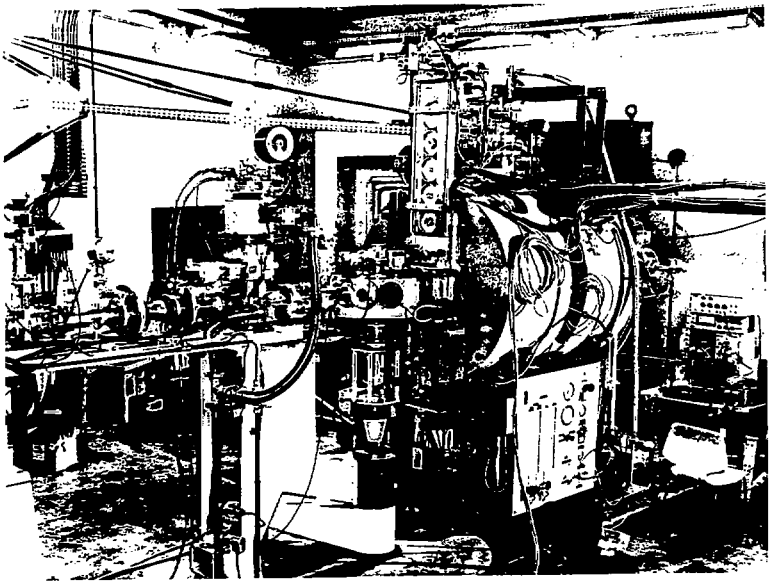

FIG. 1 : General view of SOLENO

A - Target chamber

B - Box containing five obturators, defining the minimum acceptance angle

C - Iris, defining the maximum acceptance angle

D - Faraday cup

E - Coil (length : 0.75 m, inner diameter : 0.486 m, outer diameter : 0.516 m)

F - Inner bore, diameter 0.36 m

G - Iron shield, thickness 0.08 m

H - Box for cryogenic pumping

I - Detector chamber

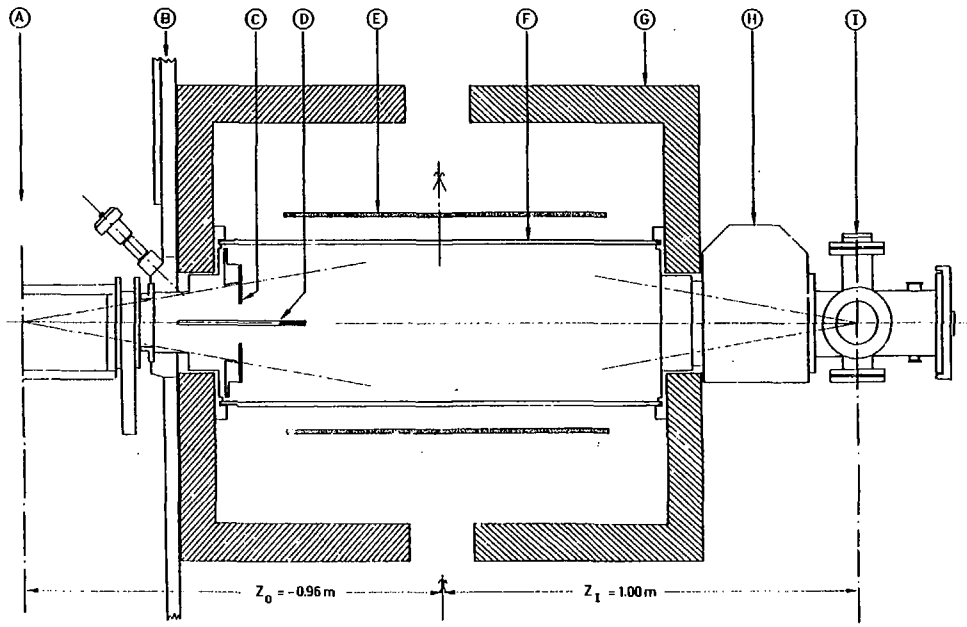

FIG. 2 : General set-up of SOLENO, with its main components (geometry A) :

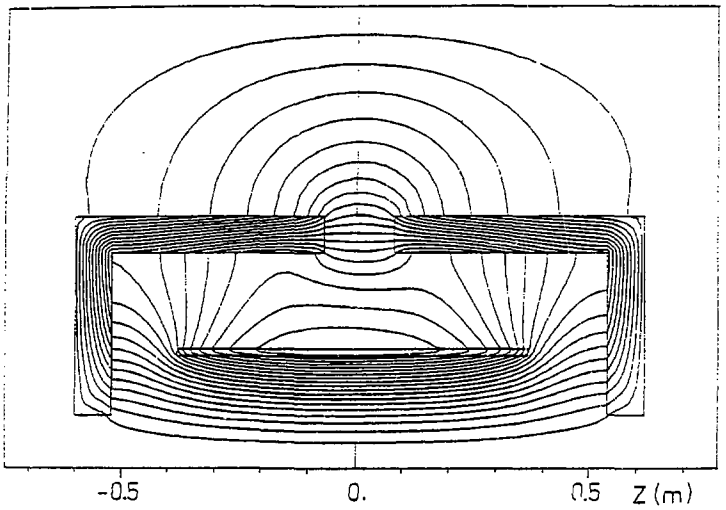

FIG. 3 : Magnetic configuration of SOLENO (TRIM calculation, see § 3)

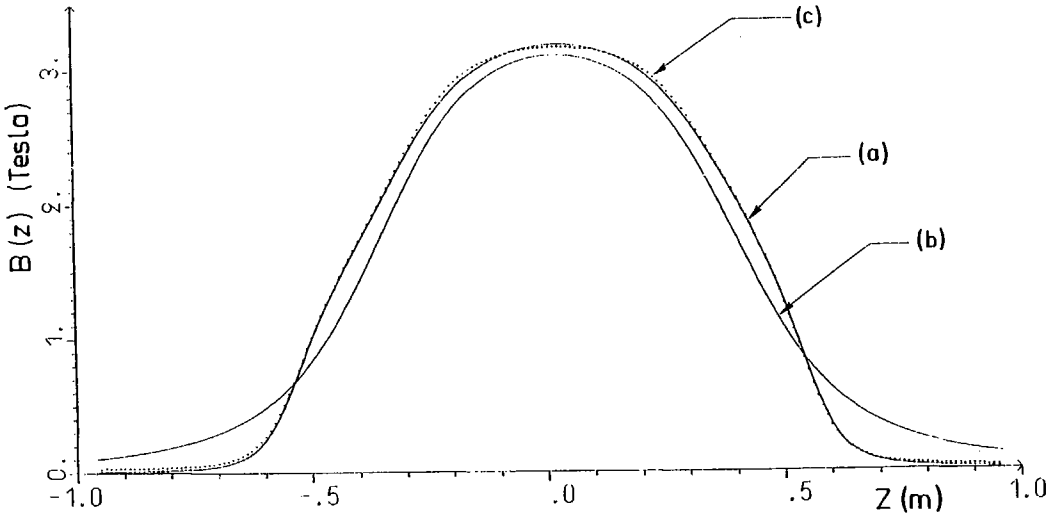

FIG. 4 : Magnetic field B(z) on axis : (a) actual magnetic field with the iron shield (b) magnetic field without any iron shield – (c) actual magnetic field measured with an Hall effect probe.

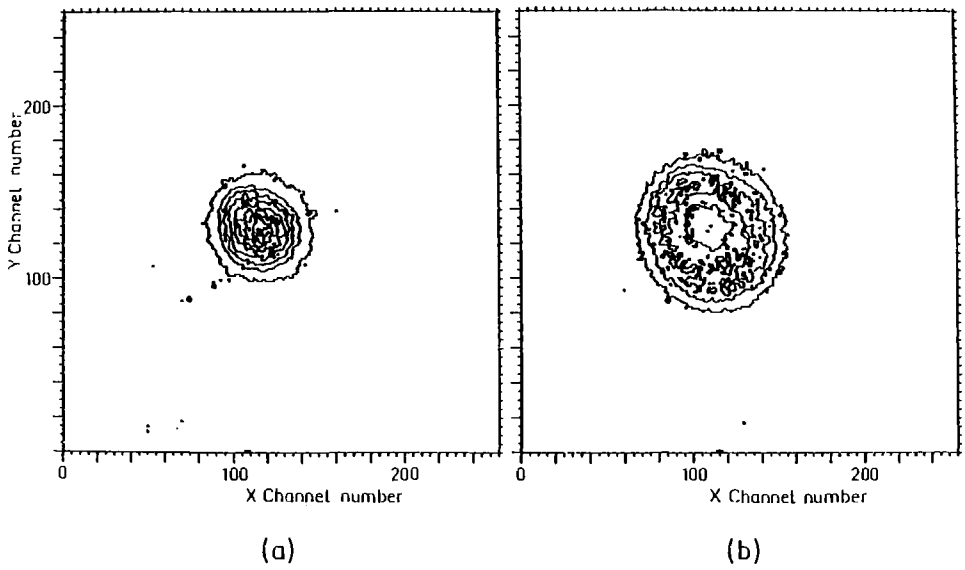

FIG. 5 : Image sizes for different Bρ settings (geometry B), using the 5.48 MeV alpha ray of ^{241}Am and a position sensitive detector, for $1° \leq \alpha \leq 6.1°$. (a) : $B\rho/\overline{B\rho} = 1.$; (b) : $B\rho/\overline{B\rho} = 1.01$ (size : 13.9 mm). In case (b) the internal circle is due to the Faraday cup.

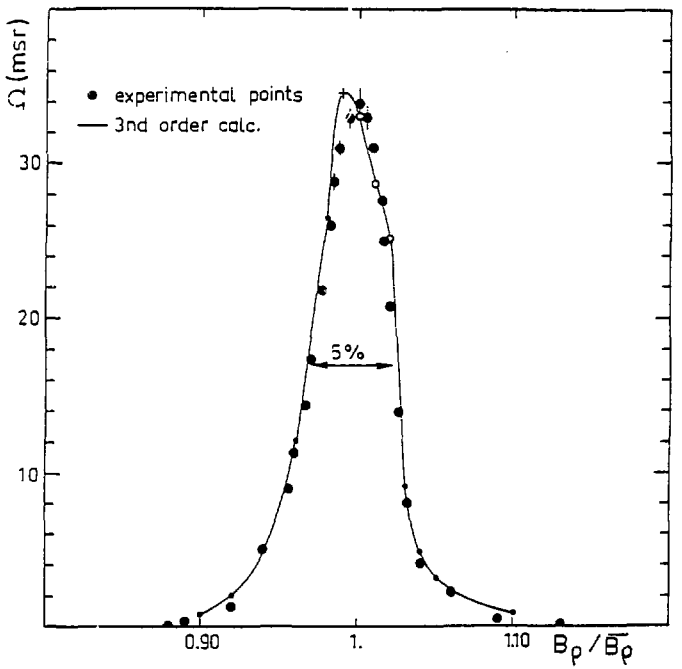

FIG. 6 : Transmission curve using a 250 mm^2 circular detector, measured with an alpha source (geometry B), and calculated in the third order approximation. In this case : • : limited by the detector size. + : limited by the entrance (6.1°) and o : limited by the exit.

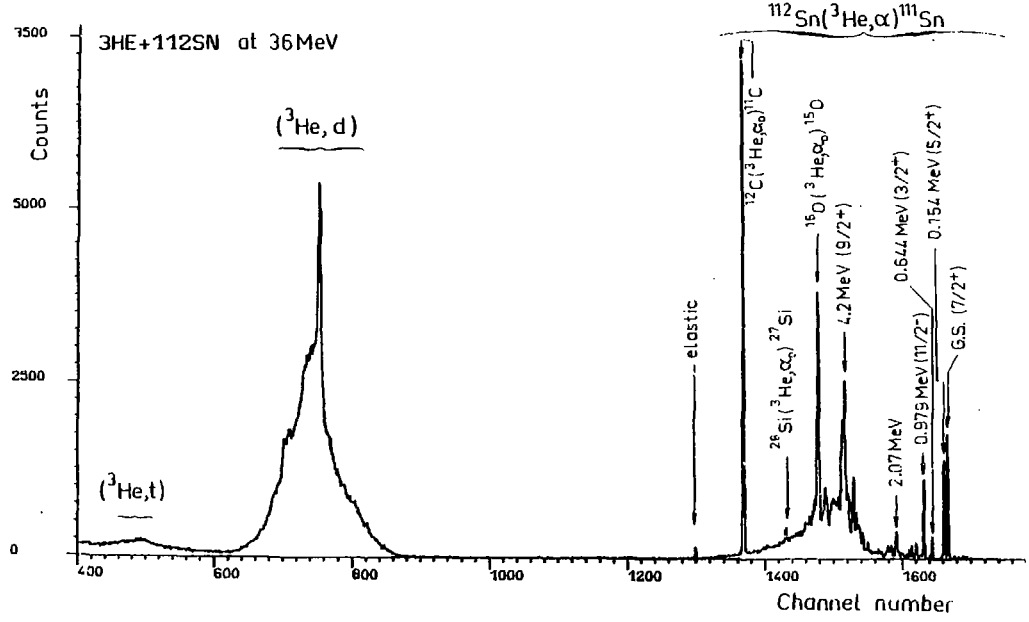

FIG. 7 : ^{3}He + ^{112}Sn spectrum at 36 MeV incident energy (see § 5). Target thickness : 350 $\mu g/cm^2$, total integrated charge 70 μC, solid angle : 28 msr (2.6° < α < 6°), $\overline{B\rho}$ = 0.930 T x m.

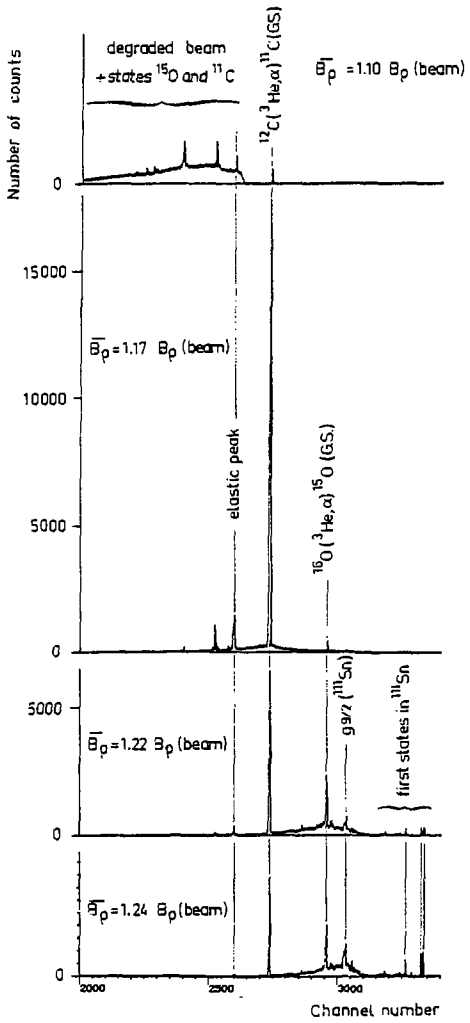

FIG. 8 : Four ^3He + ^{112}Sn spectra at 36 MeV incident energy, for different current settings of SOLENO.

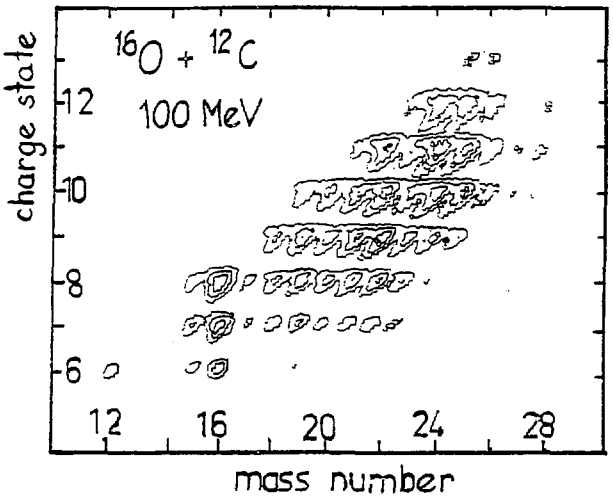

FIG. 9 : Mass and charge state spectrum in the $^{16}O + ^{12}C$ reaction at 100 MeV incident energy (^{16}O beam).

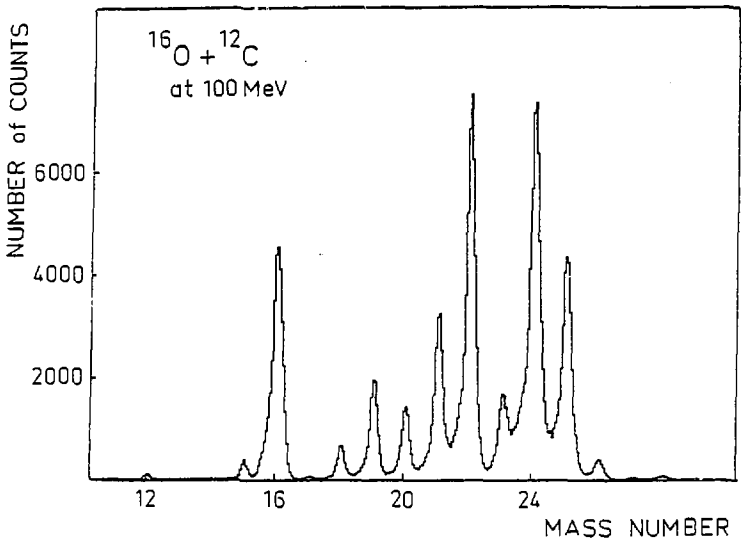

FIG. 10 Total mass spectrum obtained in the $^{16}O + ^{12}C$ reaction at 100 MeV incident energy (^{16}O beam).

TABLE I

Technical characteristics of SOLENO (First coil)

A - THE SUPERCONDUCTING WIRE

. supplier	M.C.A. (USA)
. alloy of niobium (46.5 %) - titanium	
. Cu ÷ supra	2 ÷ 1
. size (with 0.1 mm of formvar)	1.1 mm x 1.52 mm
. number of filaments	276
. diameter of filament	47 microns
. twist pitch	25 mm
. critical current at 4 Teslas at 4.2°K	950 A
. critical current at 5 Teslas at 4.2°K	800 A
. total length	9300 meters

B - THE COIL

. length	0.75 m
. inner radius	0.243 m
. thickness	0.0146 m
. weight	100 kg
. number of turns	5902
. max-current	375 A (22 800 A/cm^2)
. inductance	8.75 Henrys
. stored energy	600 kJ
. max. field at the centre	3.17 Teslas
. initial cool down delay with 40 l of LN^2	8 hours
. cool down at 4.2°K and fill up with 100 l of LHe	5 hours
. He consumption at 375 A	5 liters/hour
. He consumption in standby	3 liters/hour

C - COIL PROTECTION

. threshold of the quench detector	0.2 V and 0.05 sec
. current breaker delay time	0.15 sec
. maximum temperature rise	100°K

Only 15 % of the total energy is dumped into the protection resistance.

D - THE IRON SHIELD

. total length	1.22 m
. total diameter	1.09 m
. thickness	0.08 m
. diameter of the hole on the axis	0.23 m
. not saturated at max. induction	

E - INNER VACUUM TUBE

. inner diameter available for trajectories	0.360 m
. Faraday cup : carbon tube : diameter	0.010 m
: length	0.300 m
. min. acceptance angle due to the Faraday cup	1 deg.

TABLE 2

Optical properties of SOLENO (one coil version)

PARAMETERS	Geometry A 3rd. order calc.	Geometry B 3rd. order calc.	Geometry B α-source measurements
Position Z_0 of the target (m) [a]	-0.98	-1.19	-1.18
Max. $B\rho$ value (Txm) at I = 375 A	0.813	0.944	0.944±0.001
Max. angular acceptance α_{max} (deg)	10.	6.1	-
Max. solid angle (msr) with α_{min} = 1°	94.5	34.6	34±1
Focal distance (m)	0.498	0.685	-
Position of plane of Gauss focus (m)	1.122	1.460	-
Linear magnification	-1.110	-1.186	-1.2±0.1
Angle of rotation (deg)	94.8	81.7	85±2
Third order spherical aberration coeff. C_3 (m)	-5.20	-0.81	-
Position Z_I of the plane of best focus (m) for $\alpha < \alpha_{max}$ detector [a]	1.000	1.375	1.375
Length of light path ℓ_0 (m)	1.960	2.555	2.555
Isochronism $\Delta\ell/\ell_0/\alpha^2$ (α = 1° ; $\alpha = \alpha_{max}$)	0.60;0.78	0.60;0.71	-
Diameter of image (mm) for $\alpha < \alpha_{max}$ at $Z = Z_I$ [b]	14.3±2.2 [b]	6.0±2.4 [b]	8.3±0.1
Diameter of image (mm) for 5° < α < 6° (10.5 msr)	1.7±2.2	3.2±2.4	-
Isochronism $\Delta\ell/\ell_0$ for 5° < α < 6°	2.5×10^{-3}	2.4×10^{-3}	-

a) The origin Z = 0 is the median plan of the iron shield (see figure 1)

b) For a source of diameter ϕ = 2 mm ; the first figure is due to C_3, the second one to the size of the source (eq. 5).

TABLE 3

Experimental conditions of the preliminary $^{16}O + ^{12}C$ fusion reaction at 100 MeV incident energy

- GEOMETRICAL PARAMETERS :

Target distance Z_O (m)	- 1.005
Detection distance Z_f (m)	1.375
Distance of the scintillator from the target (m)	0.15
Minimum angle of acceptance (deg)	4.33
Maximum angle of acceptance (deg)	6.33
Solid angle (msr)	20.40
Calculated mean length l (α = 5°) of flight path (m)	2.240
Total isochronism $\Delta l/l$	4.2×10^{-3}

- SOLENO parameters

Current (Amp)	175.
$\overline{B\rho}$ setting (T x m)	0.420
$B\rho$ bandwidth (%)	5

- DETECTOR PARAMETERS

Scintillator film thickness ($\mu g\ cm^{-2}$)	250.
Surface barrier thickness (μ)	50.
Surface barrier area (mm^2)	280.

- TARGET BEAM AND PARAMETERS

Target thickness ($\mu g\ cm^{-2}$)	50.
Integrated charge (μC of O^{8+})	63.
Average current (nA of O^{8+})	60.